A Robust Machine Learning Algorithm for Cosmic Galaxy Images Classification Using Neutrosophic Score Features.

A. A. Abd El-Khalek [1], A. T. Khalil [2], M. A. Abo El-Soud [2], and Ibrahim Yasser [2,*]

[1] Communications and Electronics Engineering Department, Nile Higher Institute for Engineering and Technology Mansoura, Egypt; ayayakot94@gmail.com.
[2] Faculty of Engineering, Mansoura University, Egypt.
abeer.tawkol@mans.edu.eg; mohyldin@mans.edu.eg; and ibrahim_yasser@mans.edu.eg.

* Correspondence: ibrahim_yasser@mans.edu.eg.

Abstract: The development of galaxy images classification automated schemes is necessary to identify, classify, and study the evolution and formation of galaxies in our universe as it is one of the main challenges faced by astronomers today. Scientists can also build a deeper understanding of galaxies evolution and formation by classifying them into various classes. This paper proposed a robust novel hybrid automated intelligent algorithm based on neutrosophic techniques (NTs) and machine learning techniques for classifying the galaxy morphological astronomical images into various types of galaxies images (Hubble types) based on its features into three main classes; Elliptical, Spiral and Irregular. A nine classifiers performance was assessed based on the machine learning (ML) techniques by using a combination of a sets of morphic features (MFs); obtained from image analysis and principal component analysis (PCA) features. The results indicated that; the classifier which called, multilayer perceptron (MLP) gives the better results for the features set consisting of nine MFs and 24 PCs features among all tested cases; Mean squared error (MSE) = 0.0021; Normalized mean squared error (NMSE)= 0.0371; Correlation coefficient (r) = 0.9889, and the Error = 0.7751 with an accuracy 99.2249 %. Then, to improve the system efficiency; the neutrosophic techniques were applied in combination with the classifier that gave the best results in the previous step on the same extracted features to get a three robust component namely; membership, indeterminacy and non-membership components to fed to the neural network. The results showed that; the combination between the NTs and MLP classifier for (MFs with 4PCs) gives the best results; MSE = 0.0001; NMSE = 0.0009; r = 0.9997, and Error = 0.4212 with an accuracy about 99.5788 % in total for all chosen sets of features. The results showed the high performance of the proposed method comparing with other methods. The experimental results are performed based on a sample from (EFIGI) catalog.

Keywords: Galaxy classification, image processing, Multi-Layer Perceptron, Neutrosophic Techniques, Machine Learning Techniques.

1. Introduction

Galaxies are the areas where hydrogen transforms into luminous stars and celestial bodies that are gravitationally bound, they have different sizes, colors and shapes, it consisting of dust, gas and billions of nuclear-powered stars that also contain most chemical elements [1]. One of the most important problems for astronomers is the galaxies classification, as it can provide significant information about the evolution and origin of the universe. It is becoming an essential trouble due to the fact of astrophysicists often use vast information databases either to check present theories, or to structure a new inference to clarify the physical processes that control nature of the universe, galaxies and the star formation [2]. The morphological classification of galaxies is a system used to classify galaxies based on their appearance and their external structure by astronomers. The system created by Sir Edwin Hubble in 1936 is the most frequent classification scheme; as he divides galaxies into three main classes in accordance of their visual appearance, namely; (i) Elliptical galaxies: are without features objects, smooth, denoted by letter E followed by integer n (E0, E3, E5, and E7); (ii) Spiral galaxies: have structures like the disk and are distinguished by a flat disk contains stars in the central bulge and on the spiral arms. The usual spirals are indicated by letter S and located at the upper half (S0, Sa, Sb, Sc, and Sd). The lower half of spiral galaxies denoted by SB (SBa, SBb, and SBc) knowen as barred spiral galaxies; and (iii) Irregular galaxies: that has very irregular shapes without galactic bulges or the spiral arms of spiral galaxies are indicated by letter I (Im, and Ibm) as shown in Figure 1 [3]. This scheme is also referred to as the "Hubble Tuning Fork". This classification updated by another classification scheme called De Vaucouleurs scheme in 1959, to obtain the Revised Hubble System (RHS). In 1958 Morgan proposed further scheme and in 1960 Van Den Berghin proposed another one. NASA also provided a universal classification, called the revised morphological types [4].

Wide catalogs have been used by astronomers over recent decades to research the fundamental physics of the universe and test theories [5]. One of the most successful modern data collection projects in astronomy is Sloan Digital Sky Survey (SDSS), which uses a dedicated 2.5-m wide-angle optical telescope for spectroscopic surveys and multi-filter imaging, its data collection began in 2000 and in its final data release, it covered most of the sky area [6].
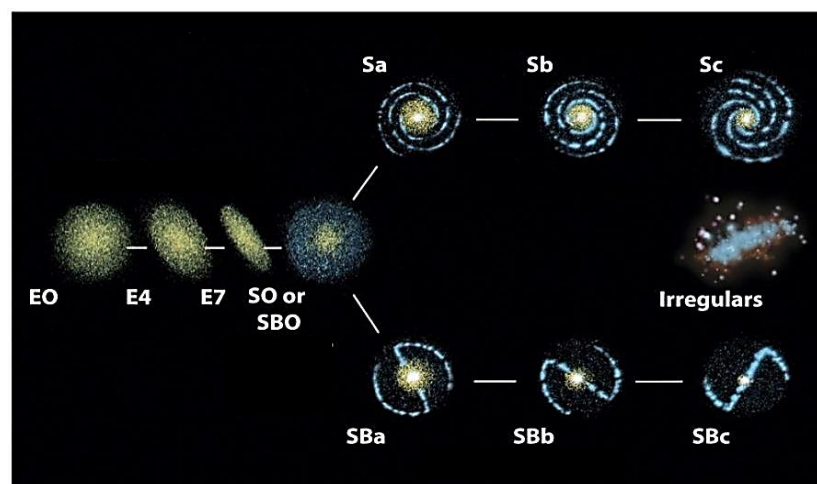

Figure 1. Hubble Galaxy Classification Scheme (Hubble 1936) [3].

Galaxies used to be manually classified into classes based on their visual characteristics in the past, however as the present-day sky surveys include images of millions of galaxies, it is found that implementing classification algorithms can assist in solving this issue. Advances in algorithms and computational tools have begun to allow galaxy morphology automated analysis by analyzing its

internal structure in the past few years. Other attempts have been made to implement the artificial neural networks using the raw pixel data as well as the image-extracted features as inputs to the artificial neural networks. To solve classical artificial intelligence issues, several deep learning algorithms have been used. All of these algorithms are a branch of machine learning techniques.

In recent years, many machine learning algorithms have played a significant role in finding solutions with classification problems, such as; Abd Elfattah et al. [7], presented Artificial Neural Network algorithms together with features extraction algorithms based on invariant moment. They have used self-organized feature maps SOFMs and time lag recurrent network TLRNs. The results showed that using SOFMs classifier have better results about 98.49 % in combination with invariant moments for feature extraction than using TLRNs classifier in combination with invariant moments about 97.29 %. Ferrari et al. [8], proposed linear discriminant analysis (LDA) to automatically classify galaxies images by measured the parameters of galaxy morphology, including asymmetry, concentration, the Gini coefficient, smoothness, entropy, spirality and moment with accuracy of more than 90%. Dieleman et al. [9], developed a rotation invariant convolutional neural network (CNN) algorithm. The achieved accuracy was approximately 99%.

Polsterer et al. [10], proposed an unsupervised method, called parallelized rotation/flipping invariant kohonen (PINK) maps to classify a number of galaxy images by extracting a set of features. This approach is focused on an enhancement of self-organizing maps with invariant similarity measure flipping and intensive rotation. Also, it is used an environment of a multi-core CPU/GPU. Selim et al. [6], presented a supervised machine learning algorithm for classifying galaxy images from the Zsoltfrei catalog based on Non-Negative matrix factorization method. The accuracy was about approximately 93% compared to other manually classified methods. Selim et al. [4], presented a new supervised machine learning algorithm for classifying galaxy images automatically from the EFIGI catalog based on the nonnegative matrix factorization method. The algorithm was used a dataset of 700 images (a large dataset) and 110 images (a small dataset). The results showed that the achieved accuracy was about 92% for large dataset and 93% for small dataset.

Aniyan et al. [11], developed a convolutional neural network (CNN) approach and 3 binary classifiers, using images from the Fanaroff–Riley (FRI and FRII) class and bent-tailed radio galaxies. The results showed that the precision is at 91%, 75% and 95% for FRI, FRII and bent-tailed radio galaxies classes, while the recall is at 91% and at 79% for each (FRI, FRIIs) and the bent-tailed class respectively. Khalifa et al. [12], proposed a CNN and a SoftMax classifier model using a sample from the EFIGI catalogue. The accuracy result was about 97.272%. Khalifa et al. [13], developed a deep convolutional neural network algorithm for galaxy images classification using EFIGI catalogue with an accuracy about 97.772%. Abd Elaziz et al. [1], proposed a new algorithm depending on the machine learning techniques using feature selection method called, artificial bee colony based on gegenbauer orthogonal moments using a sample from the EFIGI catalog. The achieved accuracy was about 94.63%. Zhu et al. [5], proposed a Residual Networks (ResNets) variant along with convolutional neural networks (CNNs) for classification of galaxy morphology. The achieved accuracy was about 95.2083%.

It is clear that prior researchers obtained successful results to some degree from the above researches. By using a new approach in the current work, the performance rate is very high by using a combination between neutrosophic techniques and machine learning based classifiers. This paper's contributions are summarized as follows:

- Building a novel hybrid automated algorithm to classify galaxies images in an efficient manner.
- Through these proposed tools, the galaxy classification process would decrease the system's complexity while achieving higher efficiencies needed to classify astronomical objects.

- Astronomers will be gaining a better understanding about the evolution of galaxies and to test many theories about the universe. In addition, they will be able to make use of the addition of this information to these catalogues of galaxies.
- Several research students will be able to use these methods in discovering new astronomical objects and use it in their projects.
- There can additionally be extension to these projects through classifying the galaxies morphology into extra than three classes.
- The excited people can add more objects of astronomical for classification, such as nebulae, stars, etc.

The paper is organized as follows: Section 2 presents the basic concepts of galaxy classification techniques. Section 3 presents the proposed approach for galaxies classification and its phases. Section 4 presents the experimental result and discussion. Finally, section 5 addresses conclusion (last section).

2. Galaxy Classification Techniques

The main objective of classification is to measure the structural characteristics of the galaxies or to distinguish between different types of these galaxies. The challenge is to create a robust automated intelligent algorithm that generates a high-performance classification which more efficient, simple, fast rating and produces higher results. There are different types of classifiers based on artificial neural networks (ANNs), nine of them were used and evaluated based on a set of selected features. We also utilized a mix between two different techniques, neutrosophic and machine learning techniques as described in the next section.

2.1 Multilayer Perceptron (MLP)

MLP is a feed forward network with layers usually trained on fixed back propagation. These networks have used into a myriad of applications that require classification of fixed patterns. Its advantages, is that any continuous and logical function can be represented as long as hidden units are suitable with using the appropriate activation function. In addition, it is simple in use, and it can round whatever output or input map [14]. MLP includes; input layer, more than a hidden layer that able to generate more efficient results and the output layer. The approach for updating weights known as back propagation in ANNs to gain the accuracy, it is aims to produce results with the least number of errors. The error is only seen at the output layer and that error is disseminated back again to preceding layers of neural network. Finally, the new weights are up to date and repetition followed again. Since the error size is large at the output layer, the same ratio of error is propagated again to the preceding layer [15].

2.2 Modular Neural Network (MNN)

MNN are a special category of MLP. It using multiple parallel MLPs, these networks process inputs and then reassemble the results. This helps to build inside the topology a certain structure, which enhances job specialization in each subunit (sub-module). Modular networks have no full connection between their layers, unlike MLP standard networks. Therefore, for the same size network, fewer weights are needed. This helps to decrease the number of necessary training models and accelerate training times. There are lots of methods to divide MLP in modules. It is not clear how the modular structure is best structured using the data [16].

2.3 Generalized Feed-Forward (GFF)

GFF networks are a generalization for MLP so that connections can leap over one or extra layers. MLP could in theory, solve any issue by the generalized forward feeding networks. However, in

practice, GFF networks addresses the issue more effectively. So, MLP takes more training cycles of hundreds of times than the GFF network comprising the same number of processing components [17].

2.4 Principal Component Analysis (PCA) Network

PCA networks combine supervised and unsupervised learning within the same structure. It is an unsupervised linear procedure finds major components and a set of uncorrelated features from the input. The nonlinear classification of these components is supervised by MLP [18].

2.5 Jordan/Elman Network (JEN)

JEN expand multi-layered perception of context units, which are processing elements which remember previous operation. Network context units offer the ability to extract the time information from the data. The output of the network is copied by the Jordan network, while the first hidden processing elements actions, are transmitted to the contextual units in the Elman network. There are also networks that feed the final hidden layer to the context units and the input [19].

2.6 Self-Organized Maps (SOMs)

SOMs networks convert the arbitrary dimension of the input into a topological (neighborhood preservation) restriction of a one- or two-dimensional discrete map. The main benefit of this network is the clustering provided by the SOM, which uses a self-organizing mechanism to reduce the input space to representative features. Then the input space basic structure is preserved, while the space dimensions are reduced. The feature maps are calculated by using unsupervised learning called Kohonen method. SOM output may be used as inputs to a supervised neural network used in classification like the network of MLP [20].

2.7 Radial Basis Function (RBF) Networks

RBF are a non-linear and hybrid networks that normally including one hidden layer of processing elements. Instead of the sigmoidal functions used by MLPs, the RBF layer using Gaussian transfer functions. The learning process of these networks is far quicker than MLPs. Gaussian's widths and centers are set by rules of non-supervised learning, and supervised learning is carried out on the output layer. All the network weights may be analytically determined if the net of generalized regression (GRNN) probabilistic (PNN) is selected. During this case, by definition, the cluster centers number and the model's number is equivalent, and the same variance is given to all of them [21].

2.8 Recurrent Networks (RNs)

RNs are the latest technology in classifying the time pattern of non-linear time series, identification of the system and prediction. Recurrent networks actually have two types: (i) partially recurrent net begin with a fully recurrent network, then it adding a feed forward connection which bypasses the recurrent portion and treating it effectively as a state memory and (ii) fully recurrent net that feedback the hidden layer to themselves. RNs may have a memory with an unlimited depth, and therefore they are finding the relationships both by the instantaneous space of input and through time [22].

2.9 Time Lagged Recurrent Networks (TLRNs)

TLRN are a multilayered perceptron networks with systems of memory of short-term. In real-world, many data consist of information in its time structure, that is, how data adjustments over time. However, most neural networks are fixed classifiers in purely. Time lagged recurrent networks are

the latest technology in classifying the time pattern of non-linear time series, identification of the system and prediction [23].

3. The Proposed Architecture

The proposed architecture framework for classification of galaxy images is presented in details in Figure 2. It includes four basic phases, (i) Preprocessing phase, followed by (ii) Feature extraction phase, (iii) Neutrosophic techniques phase, then (iv) Machine learning and Classification phase. In this section, these four phases are defined in details with the involved steps, the features and the characteristics of each phase.
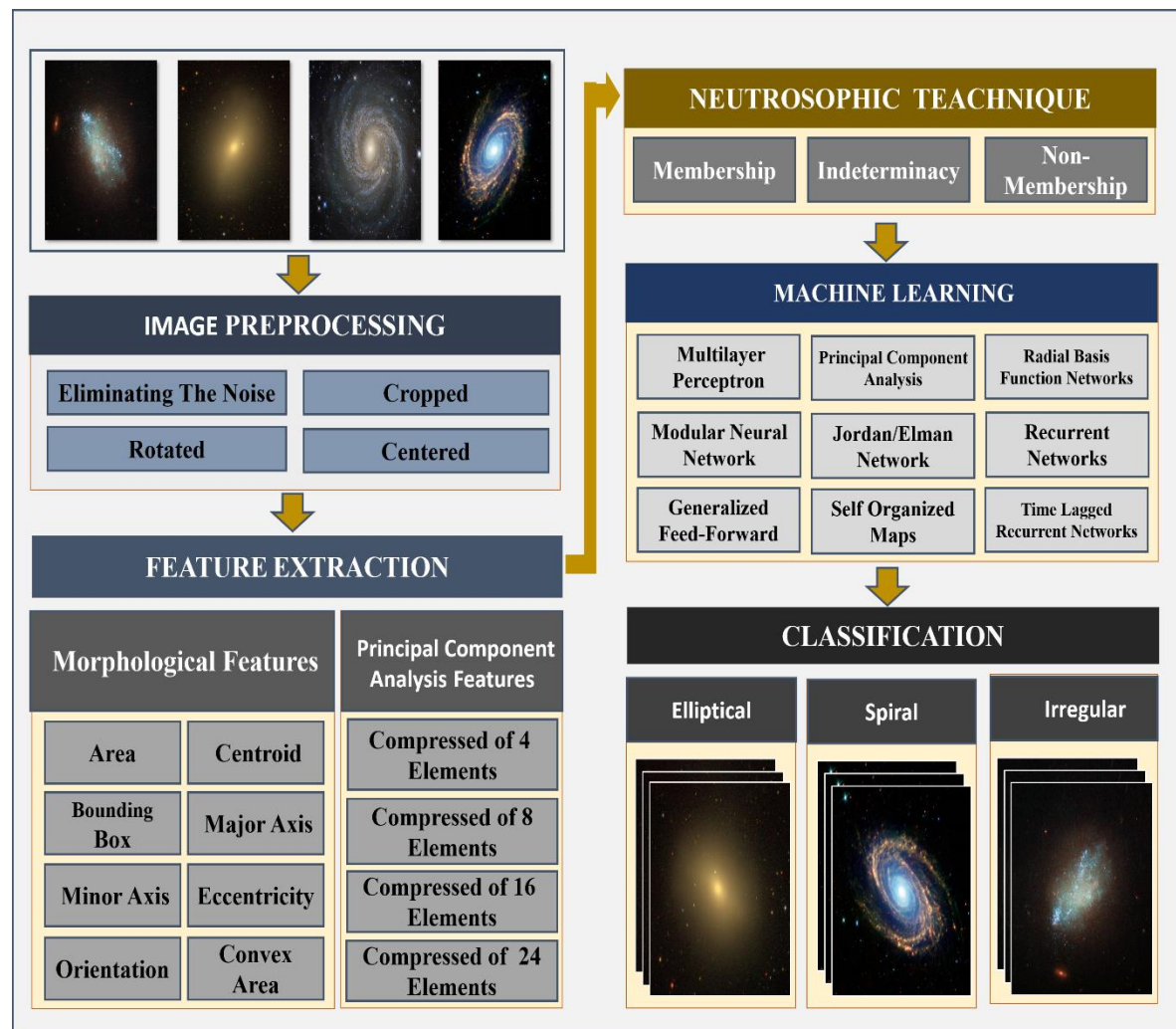

Figure 2. Visualizes The Proposed Architecture Galaxy Classification Framework.

3.1 Image Preprocessing Phase

Before extracting any features from the images, the pre-processing phase is necessary to enhance the images and also before applying the machine learning algorithm. Also, the dataset that collected is often of various sizes, colors, noise, positioning, etc. The image processing goal is to create fixed images, all of which are equal in color, noise elimination and size before feeding the images to the neural network [24].

3.2 Feature extraction phase

The extraction of features leads to some shift in the original features by performing transformations and combinations to create other more effective features by extracting the features from the entered data to improve the accuracy of learning models. This stage decreases data dimensions by removing redundant data and thus maintaining the most prominent features, as it improving the speed of training and inference. In generally, the features extraction is used to indicate the creation of linear sets of continuous features with a fine discriminatory force among categories [25]. In this paper, nine sets of morphic features (MFs) in addition to a set of principal components (PCs); (4, 8, 16 and 24) were extracted from the galaxy images, to get the efficient and the most salient features from the chosen database images.

3.2.1 Principal Component Analysis (PCA) Features

PCA is a statistical second order method which converts a number of associated variables into a smaller number of unassociated variables known as PCs. In general, principal component analysis is used to minimize the data set dimensions with maintaining as much information as possible. The data can be represented through a few base vectors instead of using all the covariance matrix PCs [26, 27]. In this paper, PCs were extracted from the whole training set; in which every image was expressed as a row vector. After that, every image coefficient was transformed into a collection of features and this is the new galaxy information representation.

3.2.2 Morphological Features (MFs)

MFs are based on the visual characteristics of the galaxy such as: (i) Minor axis: the minor ellipse axis length in pixels, which has the same natural central second moment as the area, (ii) Major axis: the major ellipse axis length in pixels, which has the same natural central second moment as the area; (iii) Orientation: expresses areas which can be described as having one dimension locally, in terms of edges or lines for example; (iv) Area: the real pixel count in the area; (v) Bounding box: shows the square with the smallest scale in which all points are located inside; (vi) Eccentricity: represents the degree to which the image of the galaxy deviates from being circular; (vii) Centroid: represents all straight lines intersection that divide the image into two equal-moment parts informally around the line, which is the average of all image points; (viii) Extrema: expresses the minimum value or the maximum value which takes in a point either in its entirety within the function domain; or within a particular neighborhood; and (ix) Convex area: represents the line segment that connects any two points within the shape, which are fully contained in the figure.

3.3 Neutrosophic Techniques (NTs) Phase

NTs are the techniques, which uses neutrosophic sets and the principles of neutrosophic logic for the classification. NTs includes a neutrosophic simple rule-based method such as: if X and Y then Z, to solve the problem rather than trying to model a mathematical similar system of fuzzy approach [28]. The architecture of the neutrosophic inference classification system using fuzzy approach is based on the fuzzy inference method principles of Mamdani [29]. The neutrosophic classification system block diagram is illustrated in Figure 3. The values of the neutrosophic components T, I and F are independent of each other. Thus, three components were constructed using MATLAB's fuzzy logic toolbox: one for the truth component of neutrosophic, the second for the component of indeterminacy and the third for the component of falsity. A correlation is drawn between the membership functions of these components in order to capture the input and output truthfulness, indeterminacy and falsity, although the operation of neutrosophic components are independent from each other [30].
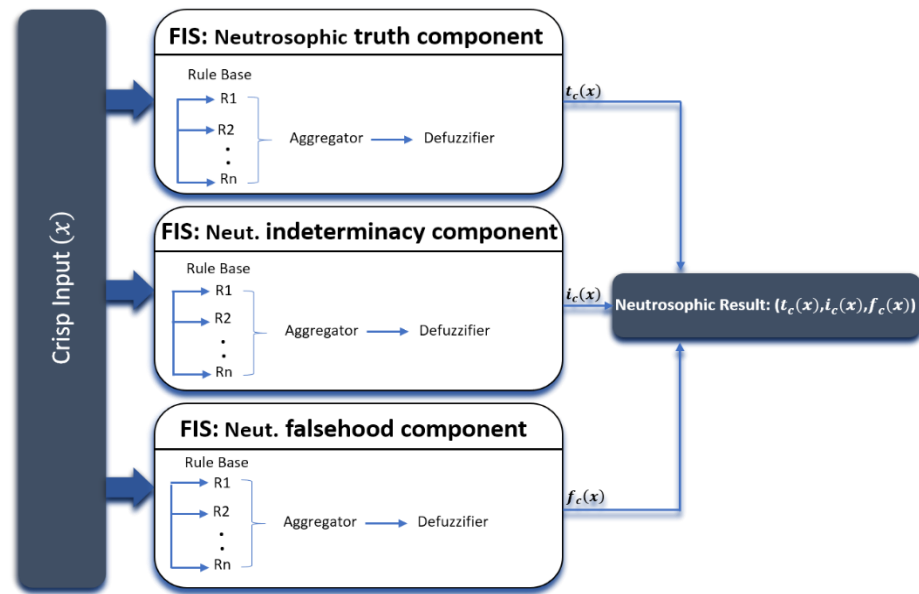
Figure 3. Block Diagram for The Neutrosophic Components [30].

The NRCS is a Neutrosophic Rule-based Classification System where neutrosophic logic is used as a method to represent various types of knowledge about the existing issue, and also to model relationships and interactions between their variables that exist [31]. Figure 4, illustrates the general structure of NRCSs.
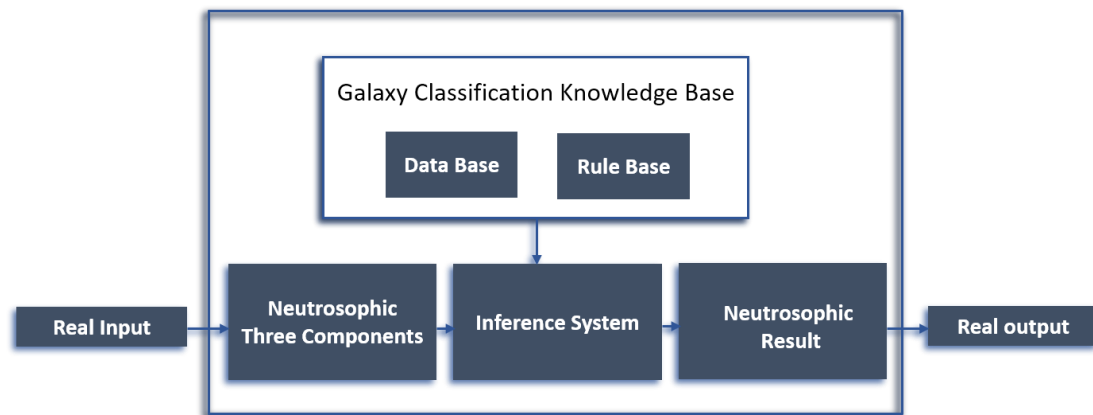

Figure 4. Basic Structure of a Neutrosophic Rule-Based Classifier System [31].

Let U be a universal set while W is a collection of bright pixels units, where W is a sub-set in U. The neutrosophic pixels sets (PNS) of images are defined by, three degrees; T, I and F. The degree of membership can be defined as T, the degree of indeterminacy can be defined as I, and the degree of non-membership can be defined as F. A pixel P in the image is defined as $P(T, I, F)$ which belonging to W with true in bright pixels (t%), indeterminate (i%) and false (f%), where t differs in T and i differs in I and f differs in F. The $p(i, j)$ pixel in domain of the image turns into:

$$NDP_{NS}(i, j) = \{T(i, j), I(i, j), F(i, j)\} \tag{1}$$

Where $NDP_{NS}(i,j)$ is the neutrosophic domain for image pixels, $T(i,j)$ belongs to white group, $I(i,j)$ belongs to indeterminate group and $F(i,j)$ belongs to non-white group. Which can be described as [32]:

$$P_{NS}(i,j) = \{T(i,j), I(i,j), F(i,j)\} \tag{2}$$

$$T(i,j) = \frac{\overline{g(\iota,J)} - \bar{g}_{min}}{\bar{g}_{max} - \bar{g}_{min}} \tag{3}$$

$$I(i,j) = 1 - \frac{H_o(i,j) - H_o}{H_{o_{max}} - H_{o_{min}}} \tag{4}$$

$$F(i,j) = 1 - T(i,j) \tag{5}$$

$$H_o(i,j) = abs\big(g(i,j)\big) - \overline{g(\iota,J)} \tag{6}$$

Where $\overline{g(\iota,J)}$ is the local mean value of window size pixels, and $Ho(i,j)$ can be described as the homogeneity value of T at (i,j), which represented with using the absolute value of the various between the intensity $g(i,j)$ and the local mean value $\overline{g(\iota,J)}$.

The neutrosophic set fundamental concepts are presented by Smarandache in [33, 34] and Salama et al. in [35-38]. In 2014, Salama et al. [39] implemented and designed an object-oriented programming [OOP] to deal with the operations of the neutrosophic data.

After extracting the features using MFs and PCA techniques, the neutrosophic techniques were used to extract three important and efficient components for every morphic and principal component feature which correlated with the most important variables for the algorithm of classification. The steps in this stage are given below, as shown in Figure 5:
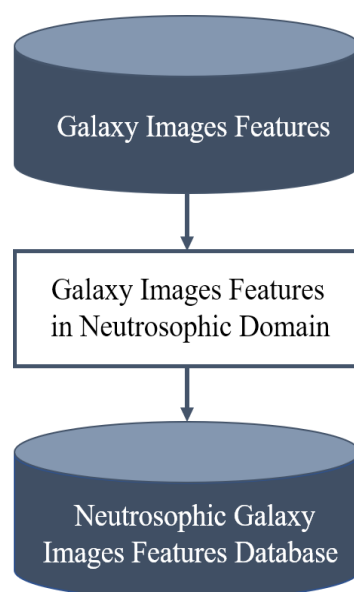

Figure 5. Neutrosophic Galaxy Images Architecture.

- Firstly, we extracted the most efficient and outstanding features to represent each image content within the database.
- Secondly, using the neutrosophic techniques, the data features have been converted from classic mode that helps with the classification process and therefore, we can make a better choice and arrange all alternatives according to three functions namely; membership, indeterminacy, and non-membership components.
- Hence, the database of neutrosophic features of galaxy images was obtained.
- finally, the three components were used to fed to the neural network to get more efficient and accurate result.

3.4 Machine learning and Classification Phase

In the machine learning and classification phase; Firstly, nine classifiers are used based on the ML techniques to conduct the learning method from the extracted features without using NTs as follows, Multilayer Perceptron (MLP), Modular Neural Network (MNN), Generalized Feed-Forward (GFF), Principal Component Analysis (PCA) Network, Jordan/Elman Network (JEN), Self-Organized Maps (SOMs), Radial Basis Function (RBF) Networks, Recurrent Networks (RNs), and Time Lagged Recurrent Networks (TLRNs). Algorithm 1, illustrates pseudo-code for the first proposed algorithm.

Algorithm 1: First Proposed Galaxy Classification Algorithm Pseudo Code

---

Begin

1) **Converting** every image from the RGB to gray scale image.
2) **Defining** the galaxy limits considering it as a nebulous object.
3) **Locating** the exact position of the galaxy by the position of the center of the spheroid bulge.
4) **Choosing** a suitable window size for eliminating the noise through property of preserving the edges.
5) **Measuring** galaxy intensity region and building a complete map for the background to subtract it from the initial image.
6) S**ubtracting** outside objects and bright stars from outside the galaxy bulge.
7) **Rotating** each galaxy image into a horizontal position.
8) **Cropping** the galaxy body from the image.
9) **Centering** the galaxy body to seem uniform.
10) **Extracting** the visual characteristics of each galaxy (Morphological features).
11) **Computing** the input data dimensions.
12) **Assuming** a galaxy image vector set (n= 255); every (n) vector has the identical length (K).
13) **Making** an n^2dimensional vector for every image.
14) **Establishing** the PCA analysis input by arranging galaxy images in a big matrix.
15) **Creating** the n dimensional matrix for every galaxy images type.
16) **Applying** the PCA algorithm, to transform these vectors to a new vector for every case of the galaxies images vectors.
17) **Computing** the mean for every type of the galaxy vector, then subtract it from every data value.
18) **Computing** the input data matrix covariance matrix (C).
19) **Calculating** the covariance matrix by choosing the largest eigenvalues (K) and the eigenvector, where (K << N).
20) **Obtaining** the new feature vector of eigenvectors of principal components.
21) **Extracting** the final data computed, i.e., the new data set.
22) I**ntroducing** the new extracted features to the ANNs based classifiers to conduct the learning Method.
23) **Obtaining** the classified galaxy images into three types of galaxies**.**

End

Then, after seeing the results we using a combination between neutrosophic techniques and machine learning based classifier including the best classifier which gave the best results in the first algorithm classification phase and it was the multilayer perceptron (MLP) classifier. After extracting the neutrosophic three components (membership, indeterminacy and non-membership) for each principal component and morphic feature in order to get more efficient and accurate result, the three components were fed to the MLP classifier, and then compared with other methods, which indicated that our method has performed better in classifying the images of galaxies to one of three types from the obtained database. Algorithm 2, illustrates pseudo-Code for the second proposed algorithm. While Figure 6 represents the MLP classifier structure model, with an illustration of the number of input layers, hidden layers, and the output layers that were used for small set of images.

Algorithm 2: Second Proposed Galaxy Classification Algorithm Pseudo Code

---

Begin

1) **Extracting** the neutrosophic three components for each principal component and morphic feature.
2) **Introducing** the extracted three components of features to the ANNs classifier to conduct the learning Method.
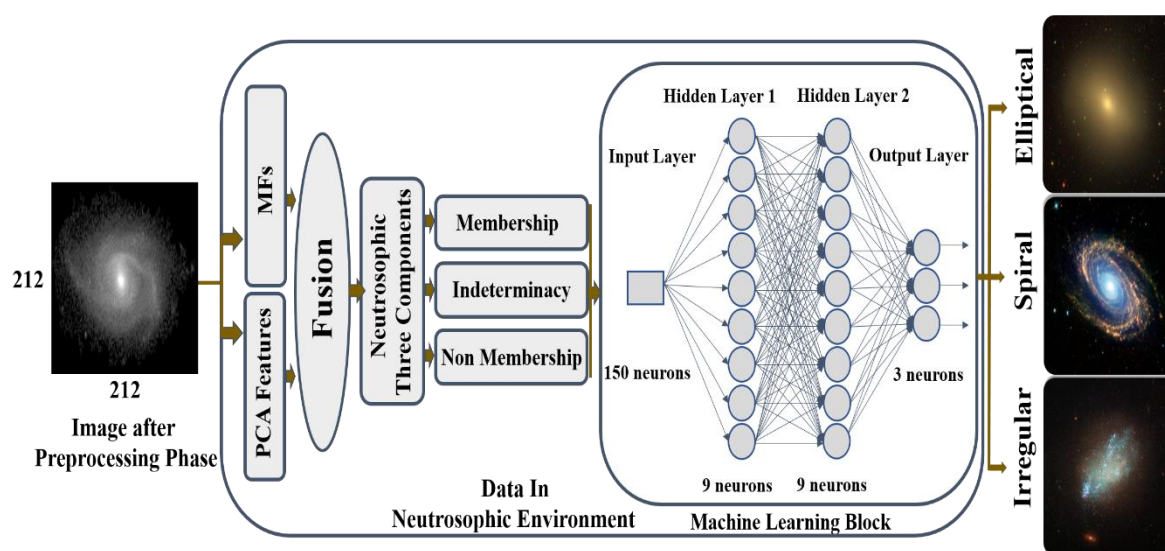3) **Obtaining** the classified galaxy images into three types of galaxies with highly efficient results.

End

Figure 6. The MLP Classifier Structure Model

4. Experimental Results and Discussion

4.1 Data set Collection

In this research, the used images were collected from the EFIGI catalog [40], the database contains a sample of all kinds of Hubble galaxies. EFIGI database are usually used in astronomical study as a benchmark, as the images are distinguished by good quality and high resolution. The catalog integrates data from standard catalogs and surveys such as (NASA Extragalactic Database, Value-Added Galaxy Catalogue, HyperLeda, Sloan Digital Sky Survey, and the Principal Galaxy Catalogue) [12]. Also, types of Hubble galaxies, such as the Elliptical, Spiral, and Irregular galaxies, were chosen according to the images captured availability. The images sizes differ in height and

width. The galaxies types and the number of training and testing images for every type of galaxy are shown in Table (1), while Figure 7 displays three samples from the galaxy images forms.

Table 1. Number of galaxy type images in each set (data, training, and testing).

Galaxy Type	Data Set	Training Set	Testing Set
Elliptical	150	105	45
Spiral	130	100	30
Irregular	110	85	25

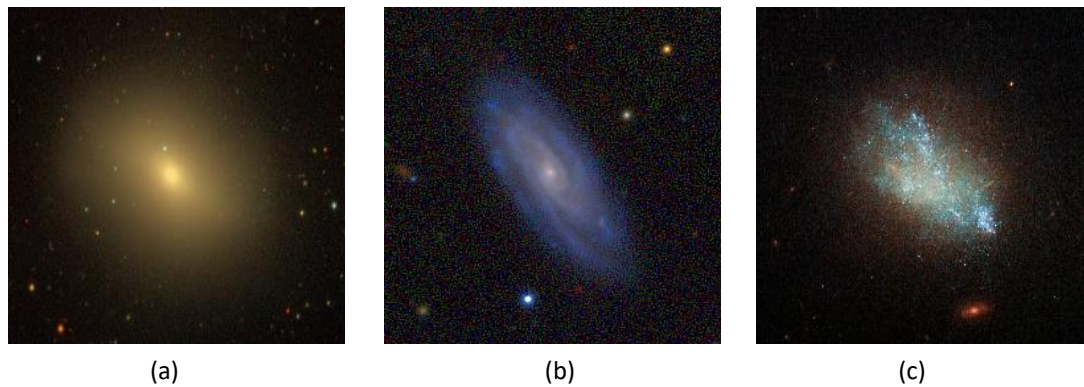(a)   (b)   (c)

Figure 7. Samples of EFIGI Catalog (a) Elliptical type, (b) Spiral type, (c) Irregular type

4.2 Performance measures

Performance measures can be characterized as a logical and mathematical structure used for calculating how near the actual results are to what was projected or predicted. The performance measures are used to compare the predictions of the trained model with the actual data from the set of test data in machine learning regression experiments. These metrics results can directly affect the process of decision-making for choosing the types of machine learning algorithms [41]. In order to assess the efficiency of the classification approach, five various performance indices metrics have been used: (i) Mean-Square Error (MSE); (ii) Normalized Mean Square Error (NMSE); (iii) Correlation Coefficient (R); (iv) Error Percentage; and (v) Accuracy. They are described as follows:

4.2.1 Mean squared error (MSE)

MSE calculates the average of the squares of the errors, i.e., the average squared difference among the values included in the estimator and the calculated quantity's actual values. MSE is a function of risk, as it Corresponding to the squared error loss' expected value. If Pij is n predictions vector, and T_i is the real values vector. MSE is calculated for the predictor as within the equation (7) [2]:

$$MSE = \frac{\sum_{j=0}^{n}(P_{ij} - T_j)^2}{n} \qquad (7)$$

where Pij is the predicted value outside of n sample cases or fitness cases measured through case i for fitness case j, while the Tj is the goal value of fitness case j.

4.2.2 Normalized mean squared error (NMSE)

NMSE is estimated the total deviations as described in the equation (8) between expected and measured values [2]:

$$NMSE = \sum_{J=0}^{n} (P_{ij} - T_j)^2 (n \times P \times T),$$ (8)

$$P = \sum_{i=1}^{n} P_{ij}/n \ and \ P = \sum_{j=1}^{n} T_j/n$$

where Pij is the predicted value outside of n sample cases or fitness cases measured through case i for fitness case j, while the Tj is the goal value of fitness case j.

4.2.3 Correlation coefficient (r)

r is the quantity which gives for the original image, the quality of the suitable least squares. The correlation coefficient is given as in equation (9) for two data sets x, y as follow [42]:

$$r = \frac{cov(x.y)}{\sigma x \times \sigma y}$$ (9)

where $cov(x.y)$ is the covariance of x and y, while σx and σy are the image (x and y) standard deviation.

4.2.4 Error percentage (Error %)

The percentage of error is determined by subtract the value that accepted from the value that calculated [42].

4.2.5 Accuracy

Accuracy is a qualitative performance characteristic, expressing the closeness of agreement between a measurement result and the value of the measurand. y_i is the corresponding true value of the predicted value and $\hat{y}_i$ is the predicted value of the $i - th$ sample. Then, the fraction of right predictions over $n_{samples}$ is defined as [5]:

$$Accuracy(y_i, \hat{y}_i) = \frac{1}{n_{samples}} \sum_{i=0}^{n_{samples}-1} 1(\hat{y}_i - y_i)$$ (10)

4.3 Results and discussion

The proposed system was trained using 390 images, with two hidden layers, and 1000 epochs, also was implemented by using (MATLAB 2017b) software package with a specific CPU and run in 64bit windows support environment. All tests were performed using a server with core i5 Intel processor 2.60 GHz, and Ram with 4.00 GB.

A. A. Abd El-Khalek; A. T. Khalil; M. A. Abo El-Soud; I. Yasser. A Robust Machine Learning Algorithm for Cosmic Galaxy Images Classification Using Neutrosophic Score Features.

In the image preprocessing phase, each image converted from the color image that contains three matrices to a gray scale image containing one matrix in order for the system to be fast and more efficient, every image of galaxy is converted as follows: **(i)** *Eliminating the image noise* by removing outside objects and bright stars by converting image to black and white (binarize image) and isolating the perimeter of the biggest object for more accurate images, **(ii)** *Rotating* every image into a horizontal position in order to have higher performance for the classifier**, (iii)** *Cropping* the galaxy body to delete those irrelevant elements from the background and selecting the image bright part, and **(iv)** *Centering* the galaxy object to seem uniform for more efficient extraction of features. *(v) Resizing* **the image** to a standard size (212 × 212) for mnimizing the origenal data dimentions. As seen in figure 8.

(a)　　　　　(b)　　　　　(c)
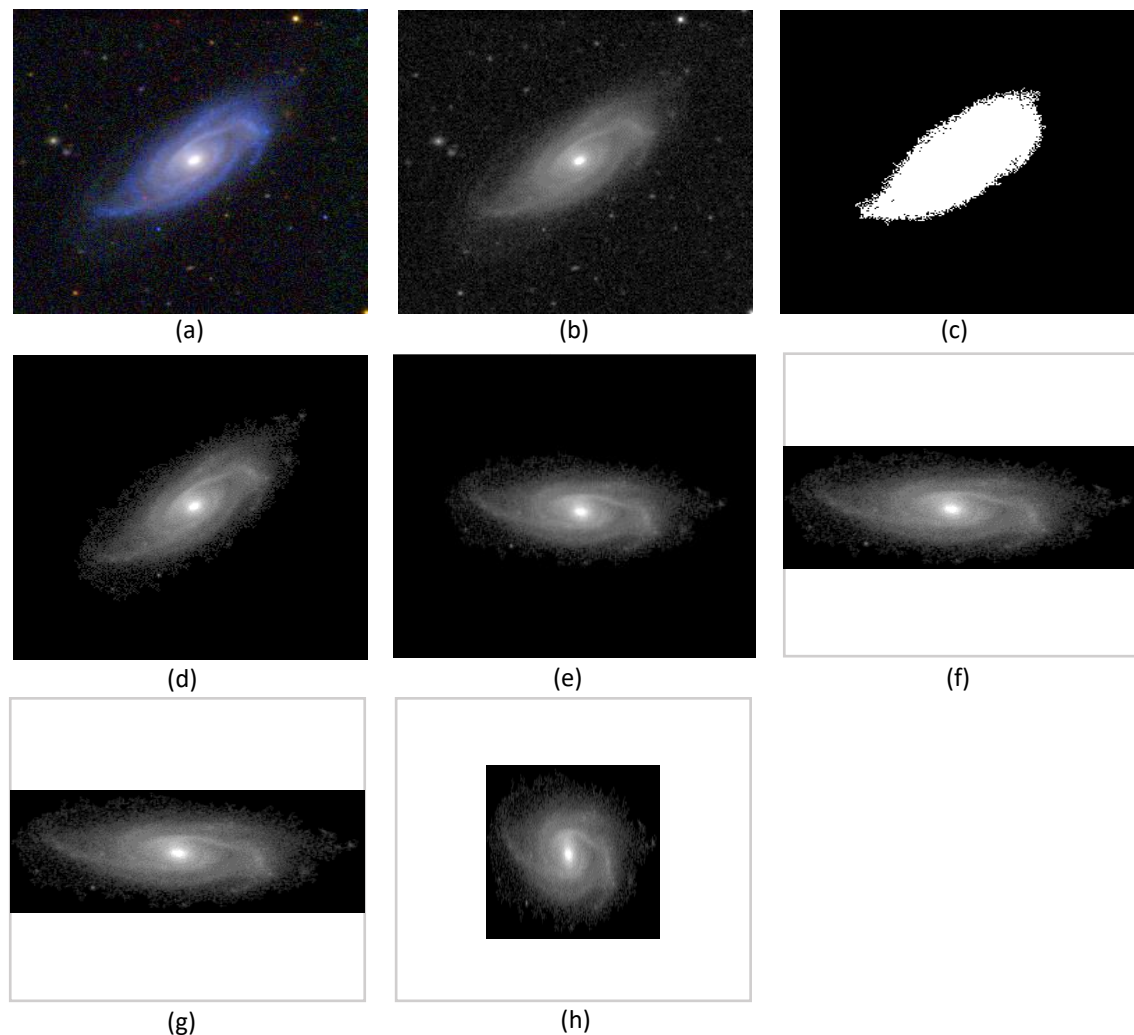
(d)　　　　　(e)　　　　　(f)

(g)　　　　　(h)

Figure 8. Spiral Galaxy (a) Raw Image, (b) Gray Scale Image, (c) Binarize Image, (d) Image without Noise, (e) Rotated Image, (f) Cropped Image, (g) Centered Image and (h) Resized Image.

The images were transformed using 4, 8, 16 and 24 element PC vector bases in the dataset as five sets of features have been organized: (i) MFs only; (ii) MFs along with 4 PCs, (iii) MFs along with 8 PCs, (iv) MFs along with 16 PCs, and (v) MFs along with 24 PCs. There is no need to extract even more PCs because the findings indicate no apparent difference with the usage of PCs greater than 24 PC. The all-tested classifiers performance, was assessed using various performance measures; MSE, NMSE, r, Error, and Accuracy. Figure 8. to Figure 12. shows the results of the nine ANN classifiers ratings discussed. The results showed the following; the MLP-based classifier using MFs only; gives

lower result from all selected features sets about; MSE = 0.1611; NMSE = 0.6011; R = 0.6131, and the Error = 4.7111 with an accuracy 95.2889% but when using the MFs with 24 PCs, the classifier performance give higher result from all chosen features sets about; MSE = 0.0021; NMSE= 0.0371; r = 0.9889, and the Error = 0.7751 with achieving an accuracy of 99.2249 % (figure 9. a., b.).

The MNN-based classifier using MFs only gives lower result from all selected features sets about; MSE = 0.2051; NMSE = 0.6991; r = 0.5901, and the Error = 5.8110 with an accuracy 94.189 % but when using the MFs with 24 PCs, the classifier performance gives higher result from all chosen features sets about; MSE = 0.1113; NMSE = 0.2605; r =0.7926, and the Error = 2.1432 with an accuracy 97.8568 % (figure 9. c., d.).
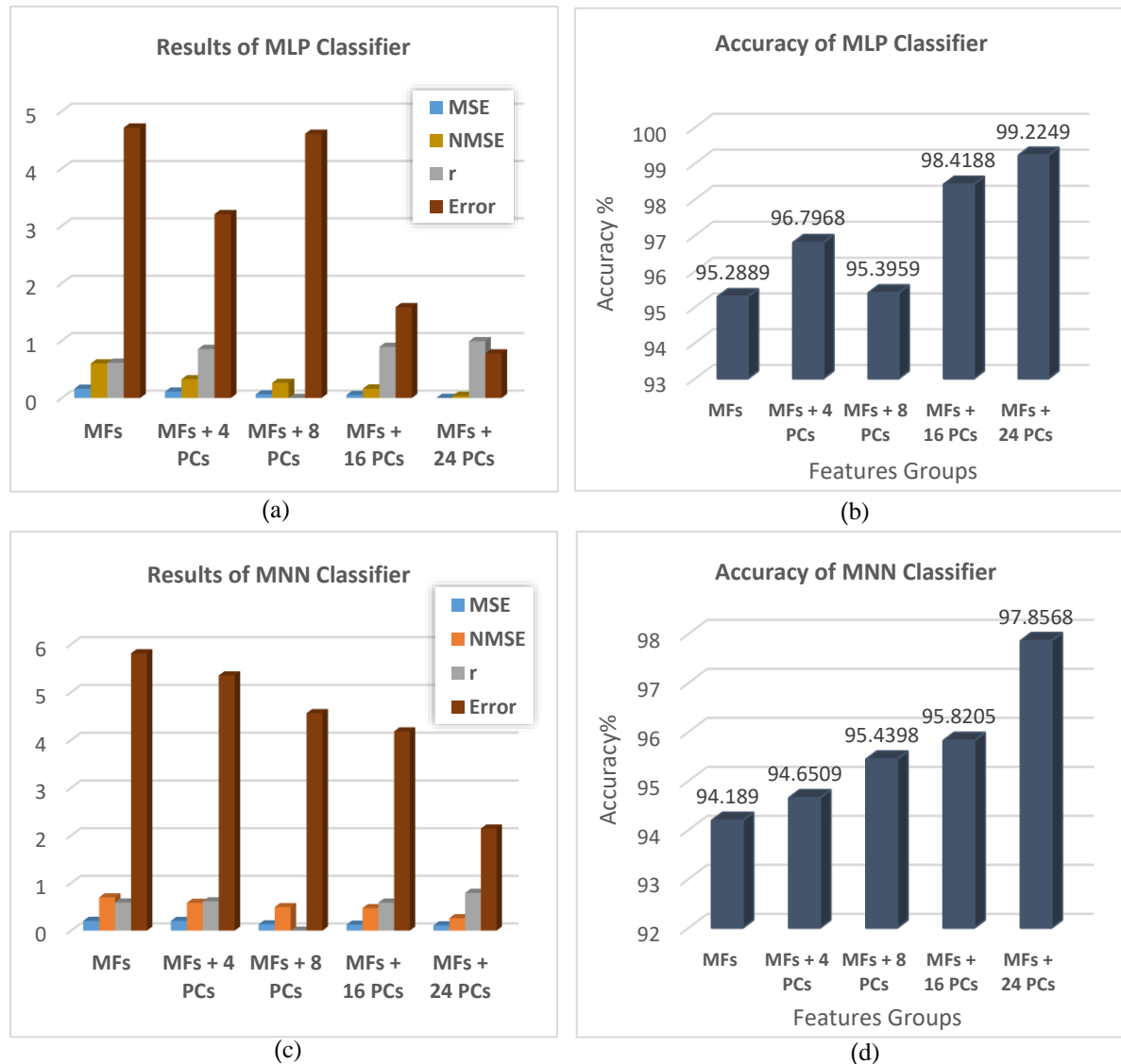

(a)

(b)

(c)

(d)

Figure 9. MLP Classification Results; (a) MSE, NMSE, r and Error, (b) Accuracy, and MNN Classification Results; (c) MSE, NMSE, r and Error, (d) Accuracy.

The GFF-based classifier using MFs only gives lower result from all selected features sets about; MSE = 0.1551; NMSE = 0.5791; r = 0.7031, and the Error = 4.6011 with an accuracy 95.3989 % but when using the MFs with 24 PCs, the classifier performance gives higher result from all chosen features sets about; MSE = 0.0119; NMSE = 0.0459; r = 0.9817, and the Error = 1.0211 with an accuracy 98.9789% (figure 10. a., b.).

The PCA-based classifier using MFs with 24 PCs gives lower result from all selected features sets about; MSE = 0.1640; NMSE = 0.6413; r = 0.3897, and the Error = 6.4533 with an accuracy 93.5467 % but when using the MFs with 4 PCs, the classifier performance gives higher result from all chosen features sets about; MSE = 0.1635; NMSE = 0.6412; r = 0.6246, and the Error = 5.4536 with an accuracy 94.5464% (figure 10. c., d.).
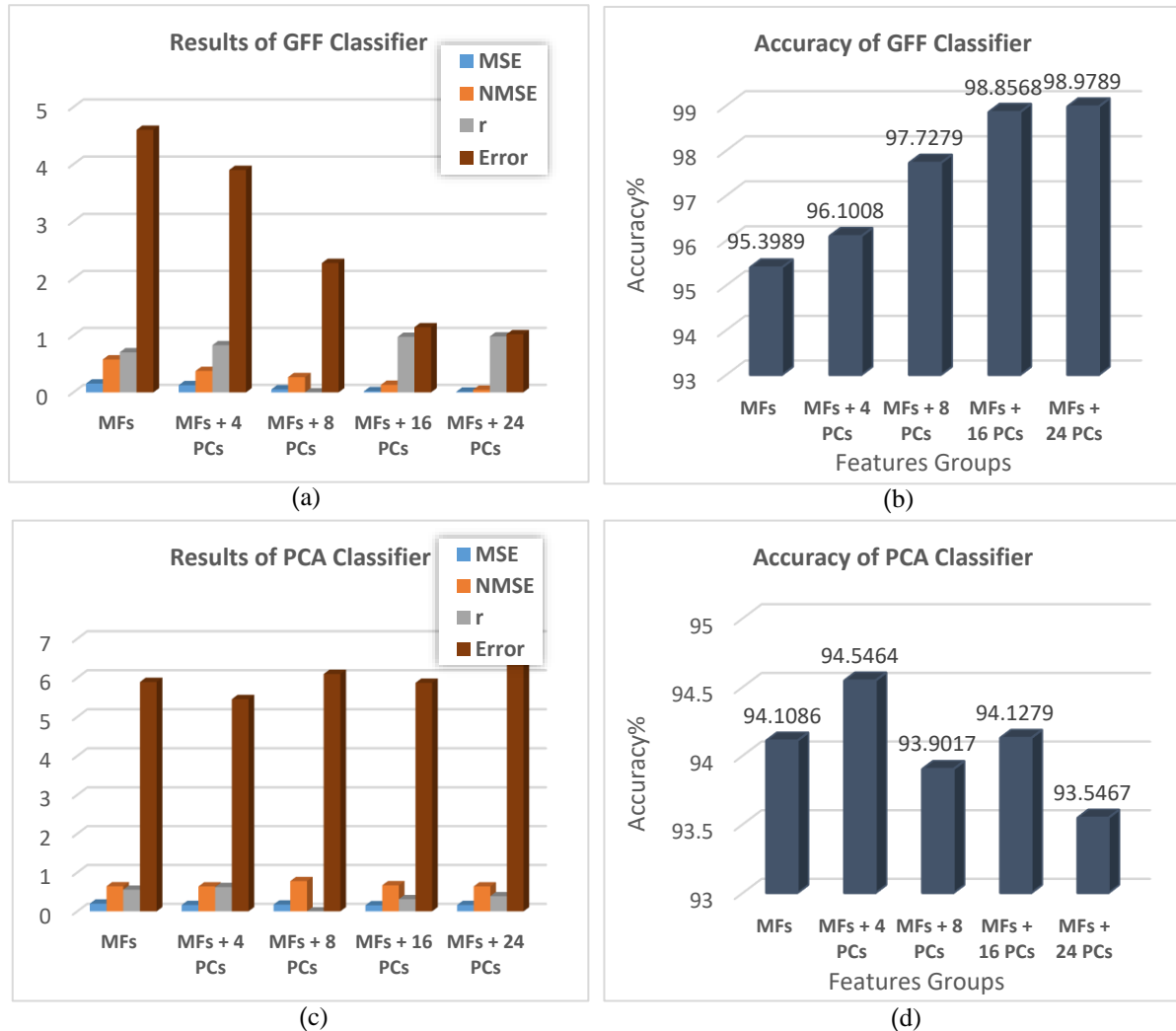

Figure 10. GFF Classification Results; (a) MSE, NMSE, r and Error, (b) Accuracy, and PCA Classification Results; (c) MSE, NMSE, r and Error, (d) Accuracy.

The JEN-based classifier using MFs only gives lower result from all selected features sets about; MSE = 0.1131; NMSE = 0.3582; r = 0.8523, and the Error = 3.7112 with an accuracy 96.2888 % but when using the MFs with 24 PCs, the classifier performance gives higher result from all chosen features sets about; MSE = 0.0136; NMSE = 0.0205; r=0.9872, and the Error = 0.9664 with an accuracy 99.0336% (figure 11. a., b.).

The SOMs-based classifier using MFs only gives lower result from all selected features sets about; MSE = 0.1235; NMSE = 0.5383; r = 0.6830, and the Error = 4.6557 with an accuracy 95.3443 % but when using the MFs with 16 PCs, the classifier performance gives higher result from all chosen features sets about; MSE = 0.1367; NMSE = 0.3541; r = 0.6247, and the Error = 3.1382 with an accuracy 96.8618 % (figure 11. c., d.).
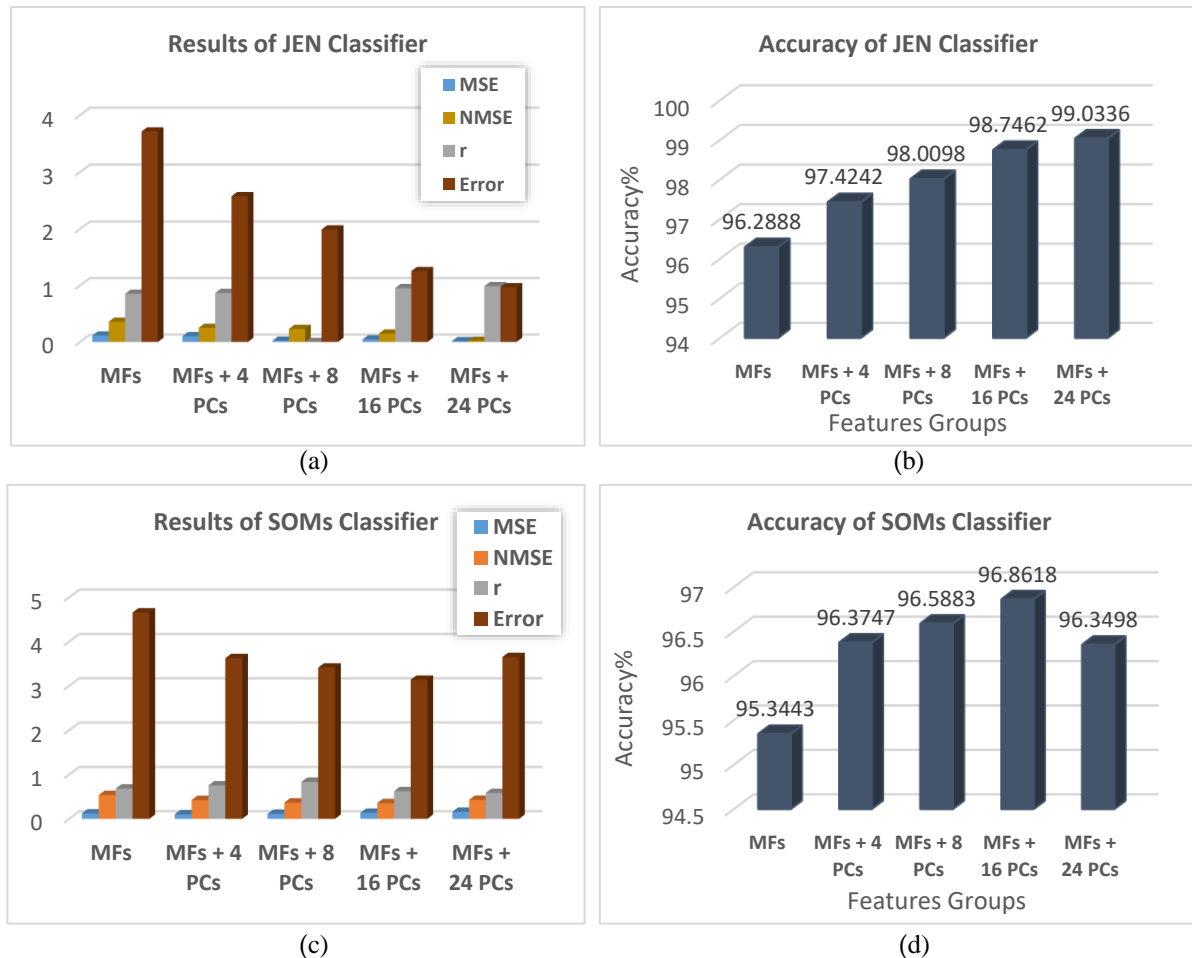
(a)

(b)

(c)

(d)

Figure 11. JEN Classification Results; (a) MSE, NMSE, r and Error, (b) Accuracy, and SOMs Classification Results; (c) MSE, NMSE, r and Error, (d) Accuracy.

The RBF-based classifier using MFs with 24 PCs gives lower result from all selected features sets about; MSE = 0.2632; NMSE = 0.8682; r = 0.1233, and the Error = 9.2390 with an accuracy 90.761% but when using the MFs only, the classifier performance gives higher result from all chosen features sets about; MSE = 0.1234; NMSE = 0.5381; r= 0.6832, and the Error = 4.6578 (figure 12. a., b.) with an accuracy 95.3422%.
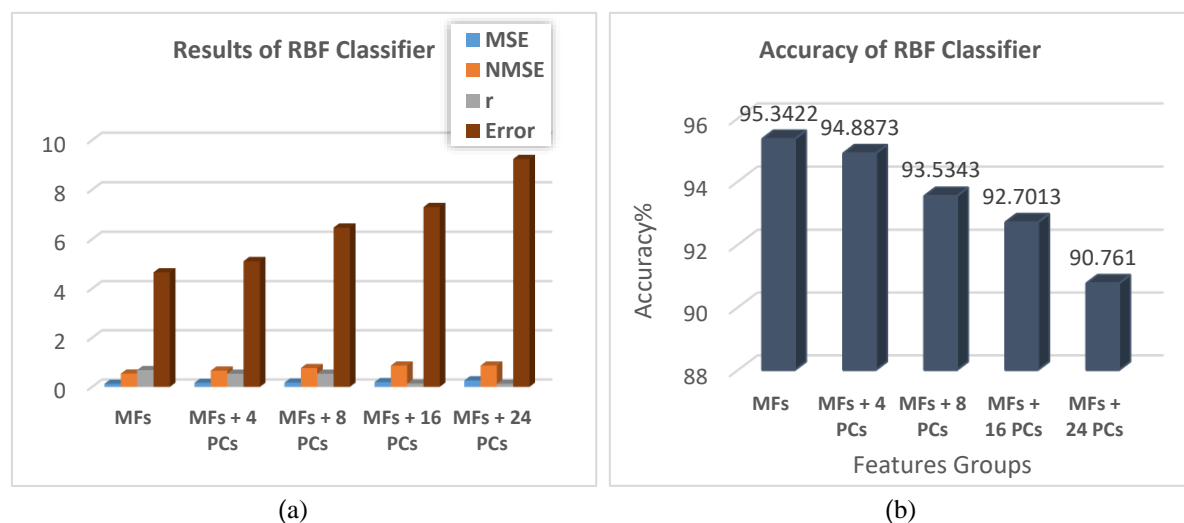

(a)

(b)

Figure 12. RBF Classification Results; (a) MSE, NMSE, r and Error, (b) Accuracy.

The RN-based classifier using MFs with 4 PCs gives lower result from all selected features sets about; MSE = 0.1998; NMSE = 0.6539; r = 0.5235, and the Error = 5.3830 with an accuracy 94.617% but when using the MFs with 24 PCs, the classifier performance gives higher result from all chosen features sets about; MSE = 0.1509; NMSE = 0.3397; r = 0.8257, and the Error = 2.4287 with an accuracy 97.5713% (figure 13. a., b.).

The TLRN-based classifier using MFs with 8 PCs gives lower result from all selected features sets about; MSE = 0.1999; NMSE = 0.5739; r = 0.5920, and the Error = 7.0739 with an accuracy 92.9261 % but when using the MFs with 16 PCs, the classifier performance gives higher result from all chosen features sets about; MSE = 0.0321; NMSE = 0.156; r = 0.9201, and the Error = 1.986 with an accuracy 98.014% (figure 13. c., d.).
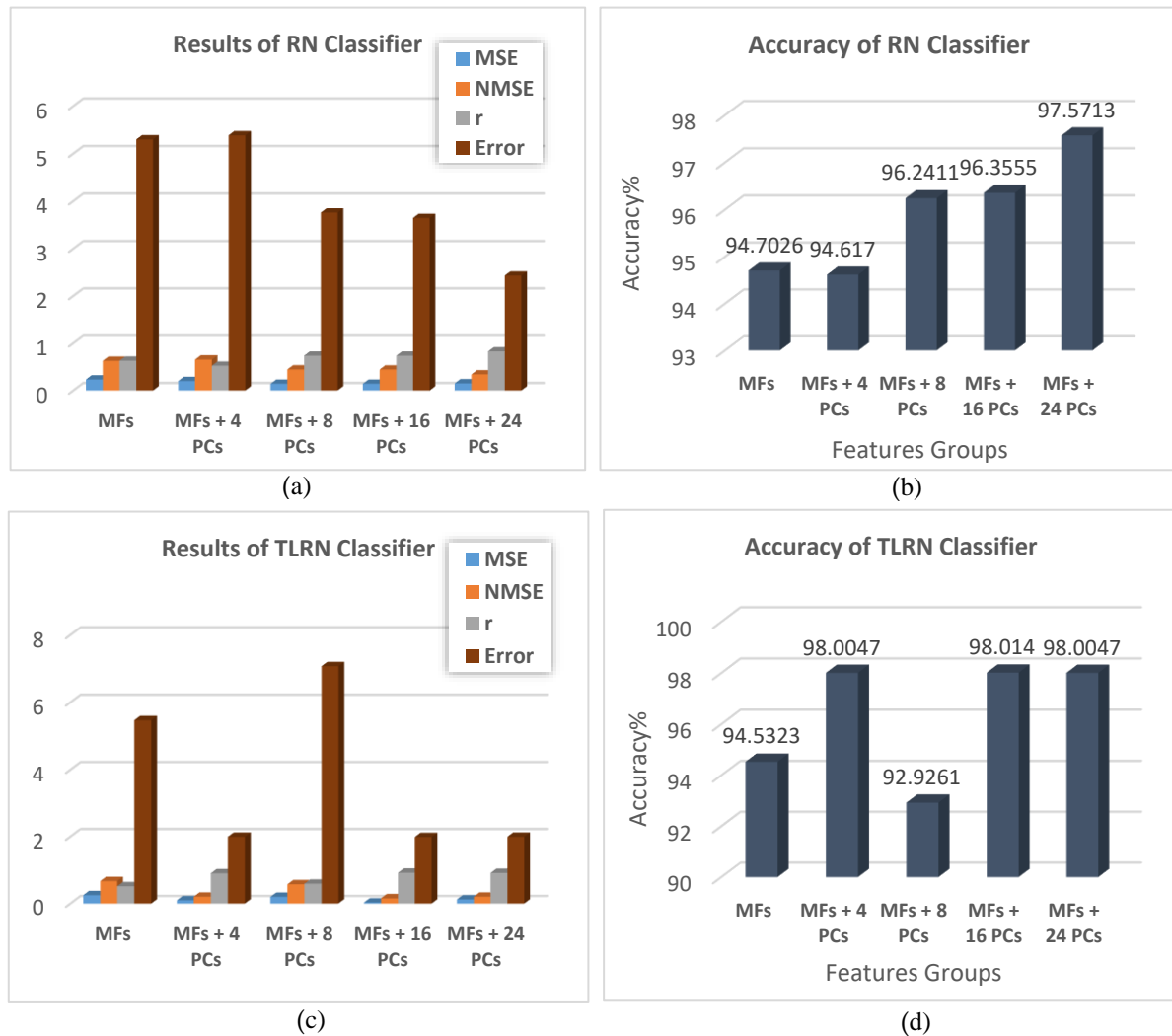

Figure 13. RN Classification Results; (a) MSE, NMSE, r and Error, (b) Accuracy, and TLRN Classification Results; (c) MSE, NMSE, r and Error, (d) Accuracy.

According to the above results, it has been found that the MLP-based classifier gives the best results for all sets of chosen features among all tested ML classifiers while, the RBF-based classifier gives the worst results.

Then, we applied the NTs in combination with the best classifier that give the best results through all tested ML classifiers (MLP). The NTs were applied on the chosen features to get a three

efficient component. Figure 14. shows the neutrosophic components (NCs) graph; membership, indeterminacy, and non-membership for the MFs along with PCs features in the neutrosophic environment.
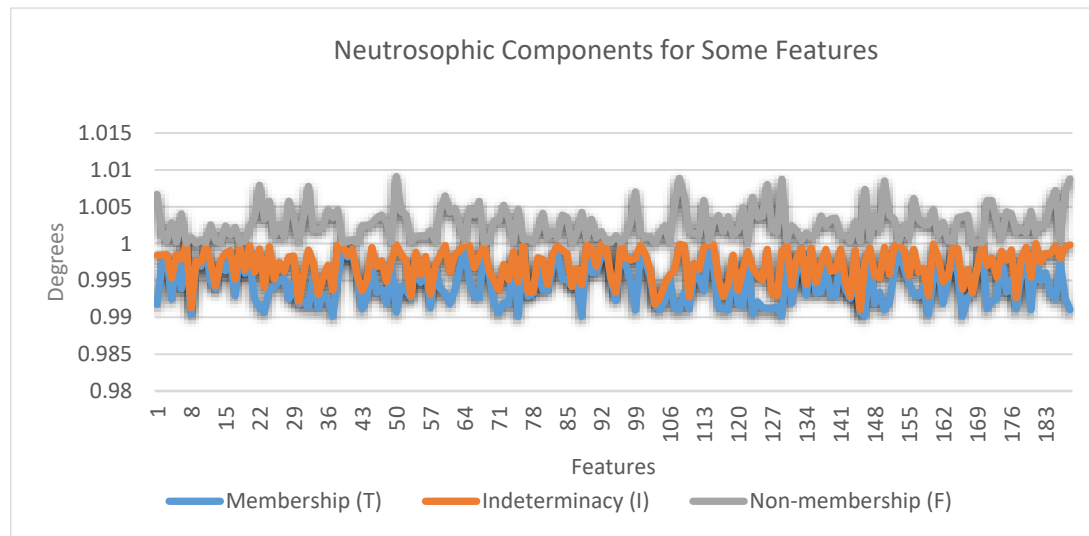

Figure 14. Neutrosophic Three Components for Some Features.

From above results, it has been found that, the MLP classifier of (MFs with 24 PCs) features gives the best results without using NTs through all tested cases for all sets of chosen features but when applied the NTs on the all tested cases for all sets of features and fed to the neural network, the results showed that; using NTs of (MFs with 4PCs) in combination with classifier of MLP gives better result than using the classifier of MLP with the other sets of features; MSE = 0.0001; NMSE = 0.0009; r = 0.9997, and Error = 0.4212 with total accuracy 99.5788 % as summarized in Table (2). The proposed system advantage is depending on a small features number that have been tested for classification, i.e., only MFs with 4PCs, and this reduces system complexity and saves time while getting higher efficiency in the classification process. This indicates, that a small set of features is enough to classify images of galaxy using the NTs. Additionally, there is no need to extract even more 4 PCs with using NTs because the results indicate no obvious difference with the use of PCs more than 4pc.

Table 2. Performance measures* of the proposed algorithm.

Performance Measures	NCs for MFs	NCs for MFs + 4 PCs	NCs for MFs + 8 PCs	NCs for MFs + 16 PCs	NCs for MFs + 24 PCs
MSE	0.0015	0.0001	0.0012	0.0014	0.0021
NMSE	0.0112	0.0009	0.0011	0.0013	0.0032
r	0.8984	0.9997	0.8988	0.9956	0.9950
Error	2.6875	0.4212	1.1743	1.4889	0.4257
Accuracy %	97.3125	99.5788	98.8257	98.5111	99.5743

* NCs: neutrosophic components, MFs: morphological features; PCs: principal components; MSE: Mean squared error; NMSE: normalized mean squared error; and r: correlation coefficient

Figure 15. represents the comparative results between the proposed system and other related works, which shows that the proposed method has high performance results for classifying galaxy images outperforms those of other related works.
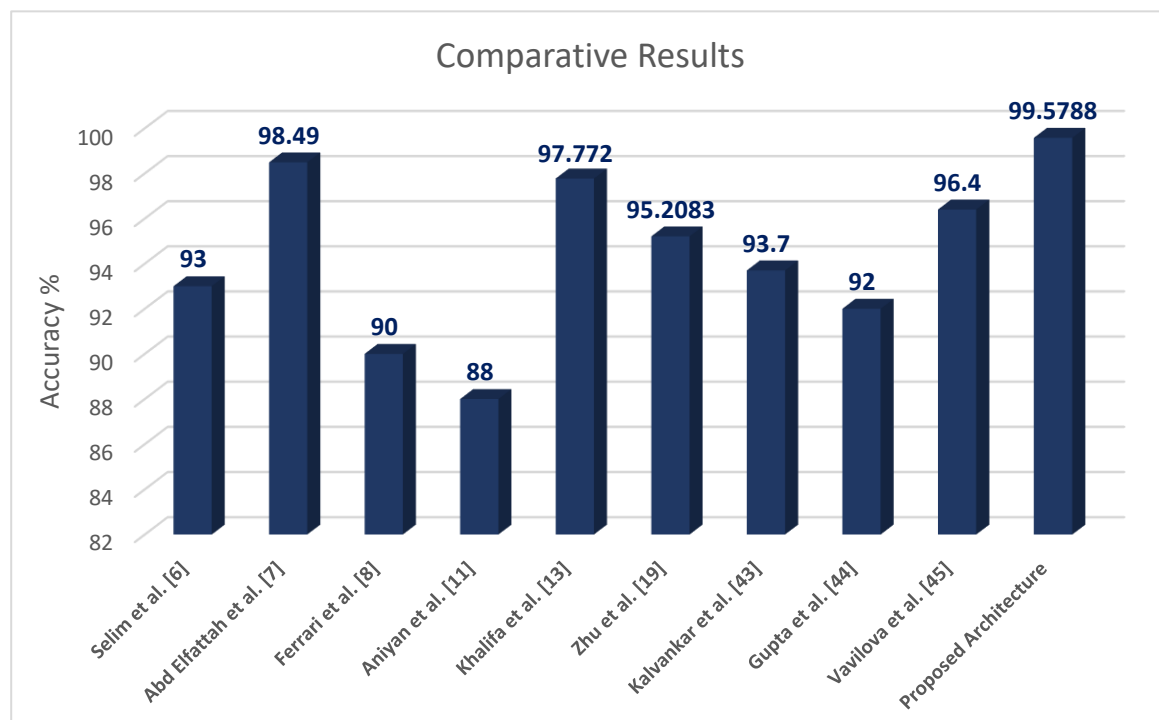

Figure 15. Comparative Accuracy Results for Galaxies Classification Comparing with Other Related Works.

The proposed algorithm achieved accuracy with 99.5788% at the testing process. Comparing with other related works, the proposed system improved the accuracy by 6.5788%, 1.0888%, 9.5788%, 11.5788%, 1.8068%, 4.3705%, 5.8788%, 7.5788%, and 3.1788% comparing with [6], [7], [8], [11], [13], [19], [43], [44], and [45], respectively. Overall, the proposed architecture provides high efficiency in addition has a high level of reliability and achieves advanced performance.

5. Conclusions

Modern sky surveys like, upcoming Large Synoptic Survey Telescope (LSST), Dark Energy Surveys (DES), and COSMOS surveys continue to generate more data, so, the classification of galaxies is one of the most important research topics and studies over the years. The main concern of research was the Hubble classification, as it allowed galaxies to be classified into one of three types based on their morphological features: Elliptical, Spiral, and Irregular. In this paper, a novel automated intelligent system for galaxy images classification into various galaxies types, which combines neural networks and their variants, machine learning algorithms and neutrosophic techniques to build more intelligent classification system was introduced. The obtained results showed that the use of MFs along with 4PCs for feature extraction in combination with NTs and the classifier of MLP gives better results compared to other methods as the testing accuracy was about 99.5788% in total and the performance measures; MSE = 0.0001; NMSE = 0.0009; r = 0.9997, and Error = 0.4212. In addition, we found that a small set of features is enough to classify images of galaxy and this necessary for reducing system complexity and saving time while getting higher efficiency in the process of classification. The results also illustrate the challenge of using the classification system on the irregular galaxies category. Since the category includes galaxies with no definite form that do not

follow the criteria of any of the other categories, the category within the set of features is difficult to classify and less diagnostic. Therefore, it is confused with other objects frequently. In upcoming surveys; our algorithm can be applied to a large-scale galaxy classification.

References

1. Abd Elaziz, M., Hosny, K.M. and Selim, I. M. (2019). Galaxies image classification using artificial bee colony based on orthogonal Gegenbauer moments. Soft Computing, 23(19), 9573-9583.

2. Abd Elfattah, M., Elbendary, N., Elminir, H.K., El-Soud, M.A.A. and Hassanien, A.E. (2014). Galaxies image classification using empirical mode decomposition and machine learning techniques. In 2014 International Conference on Engineering and Technology (ICET), IEEE, 1-5.

3. Sharma, P. and Baral, A. (2018). Galaxy Classification Using Neural Networks: A Review. In 2018 International Conference on Audio, Language and Image Processing (ICALIP), IEEE, 179-183.

4. Selim, I.M. and Abd El Aziz, M. (2017). Automated morphological classification of galaxies based on projection gradient nonnegative matrix factorization algorithm. Experimental Astronomy, 43(2), 131-144.

5. Zhu, X.P., Dai, J.M., Bian, C.J., Chen, Y., Chen, S. and Hu, C. (2019). Galaxy morphology classification with deep convolutional neural networks. Astrophysics and Space Science, 364(4), 55.

6. Selim, I., Keshk, A.E. and El Shourbugy, B.M. (2016). Galaxy image classification using non-negative matrix factorization. Int. J. Comput. Appl, 137(5), 4-8.

7. Abd Elfattah, M., El-Bendary, N., Elsoud, M.A.A., Hassanien, A.E. and Tolba, M.F. (2013). An intelligent approach for galaxies images classification. In 13th International Conference on Hybrid Intelligent Systems (HIS 2013), IEEE, 167-172.

8. Ferrari, F., de Carvalho, R.R. and Trevisan, M. (2015). Morfometryka—a new way of establishing morphological classification of galaxies. The Astrophysical Journal, 814(1), 55.

9. Dieleman, S., Willett, K.W. and Dambre, J. (2015). Rotation-invariant convolutional neural networks for galaxy morphology prediction. Monthly notices of the royal astronomical society, 450(2), 1441-1459.

10. Polsterer, K.L., Gieseke, F. and Igel, C. (2015). Automatic galaxy classification via machine learning techniques: Parallelized rotation/flipping INvariant Kohonen maps (PINK). Astronomical data analysis software and systems XXIV (ADASS XXIV), vol 495, p 81.

11. Aniyan, A.K. and Thorat, K. (2017). Classifying radio galaxies with the convolutional neural network. The Astrophysical Journal Supplement Series, 230(2), 20.

12. Khalifa, N.E.M., Taha, M.H.N., Hassanien, A.E. and Selim, I.M. (2017). Deep galaxy: Classification of galaxies based on deep convolutional neural networks. arXiv preprint arXiv:1709.02245.

13. Khalifa, N.E., Taha, M.H., Hassanien, A.E. and Selim, I. (2018). Deep galaxy V2: Robust deep convolutional neural networks for galaxy morphology classifications. In 2018 International Conference on Computing Sciences and Engineering (ICCSE), IEEE, 1-6.

14. Mohamed, M.A. and Atta, M.M. (2010). Automated classification of galaxies using transformed domain features. Int. J. Comput. Sci. Network Security, 10, pp.86-91.

15. Biswas, M. and Adlak, R. (2018). Classification of Galaxy Morphologies using Artificial Neural Network. In 2018 4th International Conference for Convergence in Technology (I2CT), IEEE, 1-4.

16. Lobato, Justo, Pablo Cañizares, Manuel A. Rodrigo, Ciprian-George Piuleac, Silvia Curteanu, and José J. Linares. "Direct and inverse neural networks modelling applied to study the influence of the gas diffusion layer properties on PBI-based PEM fuel cells." international journal of hydrogen energy 35, no. 15 (2010): 7889-7897.

17. Abdel-Azim, Mohamed, A. I. Abdel-Fatah, and Mohamed Awad. "Performance analysis of artificial neural network intrusion detection systems." In 2009 International Conference on Electrical and Electronics Engineering-ELECO 2009, pp. II-385. IEEE, 2009. .

18. Hsieh, W.W., 2001. Nonlinear principal component analysis by neural networks. Tellus A, 53(5), 599-615.

19. Dhule, V., Pathare, S., Sadaphale, R. and Tekade, A., Comparison of ANN Networks Using Parks-Hilbert Approach.

20. Yin, H., 2008. The self-organizing maps: background, theories, extensions and applications. In Computational intelligence: A compendium (pp. 715-762). Springer, Berlin, Heidelberg.

21. Markopoulos, A.P., Georgiopoulos, S. and Manolakos, D.E. (2016). On the use of back propagation and radial basis function neural networks in surface roughness prediction. Journal of Industrial Engineering International, 12(3), pp.389-400.

22. Atiya, A.F. and Parlos, A.G. (2000). New results on recurrent network training: unifying the algorithms and accelerating convergence. IEEE transactions on neural networks, 11(3), pp.697-709.

23. Liang, Y. and Kelemen, A., (2009). Time lagged recurrent neural network for temporal gene expression classification. International Journal of Computational Intelligence in Bioinformatics and Systems Biology, 1(1), 86-99.

24. Bastanfard, A. and Amirkhani, D. (2019). Automatic Classification of Galaxies Based on SVM. In 2019 9th International Conference on Computer and Knowledge Engineering (ICCKE), IEEE, pp. 32-39.

25. Khalid, S., Khalil, T. and Nasreen, S. (2014). A survey of feature selection and feature extraction techniques in machine learning. In 2014 Science and Information Conference (pp. 372-378). IEEE.

26. Cateni, S., Vannucci, M., Vannocci, M. and Colla, V. (2012). Variable selection and feature extraction through artificial intelligence techniques. Multivariate Analysis in Management, Engineering and the Science, pp.103-118.

27. Mankar, V.R. and Ghatol, A.A. (2009). Design of Adaptive Filter Using Jordan/Elman Neural Network in a Typical EMG Signal Noise Removal. Advances in artificial neural systems Vol. 2009, p. 9.

28. Ansari, A.Q., Biswas, R. and Aggarwal, S. (2013). Neutrosophic classifier: An extension of fuzzy classifer. Applied soft computing, 13(1), 563-573.

29. Mohammed, M. N., Syamsudin, H., Al-Zubaidi, S., AKS, R. R., Yusuf, E. (2020). Novel COVID-19 detection and diagnosis system using IOT based smart helmet. International Journal of Psychosocial Rehabilitation, 24 (7), 2296- 2303.

30. Yasser, I., Twakol, A., El-Khalek, A. A., Samrah, A. and Salama, A.A. (2020). COVID-X: Novel Health-Fog Framework Based on Neutrosophic Classifier for Confrontation Covid-19. Neutrosophic Sets and Systems, 35(1), p.1.

31. Fang, Y., Zhang, H., Xie, J., Lin, M., Ying, L., Pang, P., and Ji, W. (2020). Sensitivity of chest CT for COVID-19: comparison to RT-PCR. Radiology, p.200432.

32. Salama, A. A., Smarandache, F., Eisa, M. (2014). Introduction to image processing via neutrosophic techniques. Neutrosophic Sets and Systems, vol. 5, 59-64.

33. Smarandache, F. (2002). Neutrosophy and neutrosophic logic. In First International Conference on Neutrosophy, Neutrosophic Logic, Set, Probability, and Statistics University of New Mexico, Gallup, NM, Vol. 87301, 338-353.

34. Smarandache, F. (1999). A unifying field in Logics: Neutrosophic Logic. In Philosophy, American Research Press, 1-141.

35. ELwahsh, H., Gamala, M., Salama, A.A. & El-Henawy, I.M. (2017). Modeling Neutrosophic Data by Self-Organizing Feature Map: MANETs Data Case Study. Procdica Computer science, 121, 152-159.

36. Salama, A.A., Eisa, M., ElGhawalby, H. and Fawzy, A.E. (2019). A New Approach in Content-Based Image Retrieval Neutrosophic Domain. In Fuzzy Multi-criteria Decision-Making Using Neutrosophic Sets, Springer, Cham., vol 369 , 361-369.

37. Salama, A.A. and Smarandache, F. (2015). Neutrosophic crisp set theory. Infinite Study. Education Publishing 1313 Chesapeake, Avenue, Columbus, Ohio 43212.

38. Salama, A.A., Abdelfattah, M., El-Ghareeb, H.A. and Manie, A.M. (2014). Design and implementation of neutrosophic data operations using object-oriented programming. International Journal of Computer Application, 5(4), 163-175.

39. Salama, A.A., El-Ghareeb, H. A., Manie, A. M., and Smarandache, F. (2014). Introduction to Develop Some Software Programs for Dealing with Neutrosophic Sets. Neutrosophic Sets and Systems, 3, 51-52.

40. De Lapparent, V., Baillard, A. and Bertin, E. (2011). The EFIGI catalogue of 4458 nearby galaxies with morphology-II. Statistical properties along the Hubble sequence. Astronomy & Astrophysics, 532, p.A75.

41. Botchkarev, A. (2019). A NEW TYPOLOGY DESIGN OF PERFORMANCE METRICS TO MEASURE ERRORS IN MACHINE LEARNING REGRESSION ALGORITHMS. Interdisciplinary Journal of Information, Knowledge & Management, 14.

42. Elfattah, M.A., El-Bendary, N., Abou Elsoud, M.A., Platoš, J. and Hassanien, A.E. (2014). Principal component analysis neural network hybrid Classification Approach for Galaxies Images. In Innovations in Bio-inspired Computing and Applications, Springer, Cham, 225-237.

43. Kalvankar, S., Pandit, H. and Parwate, P., (2020). Galaxy Morphology Classification using EfficientNet Architectures. arXiv preprint arXiv:2008.13611.

44. Gupta, R., Srijith, P.K. and Desai, S., (2020). Galaxy Morphology Classification using Neural Ordinary Differential Equations. arXiv preprint arXiv:2012.07735.

45. Vavilova, I.B., Dobrycheva, D.V., Vasylenko, M.Y., Elyiv, A.A., Melnyk, O.V. and Khramtsov, V., (2021). Machine learning technique for morphological classification of galaxies from the SDSS. I. Photometry-based approach.